Division of Materials Sciences and Engineering
Office of Basic Energy Sciences
US Department of Energy

1. DOE award # and name of the recipient (Institution)

DE-SC0014450, Virginia Polytechnic Institute and State University

2. Project Title and name of the PI

Mesoscale Design of Magnetoelectric Nanocomposites
Dwight Viehland (PI)
Shashank Priya (co-PI)

3. Date of the report and period covered by the report

September 2016
August 1, 2015 – July 31, 2016

4. A brief description of accomplishments. This can be in bullet form or whatever you think is useful and appropriate to indicate the sense of progress. Please limit this section to no more than 5 pages.

This is a final report for a transient program that was issued to Virginia Tech as a new program (DE-SC0001450), rather than as a renewal to our existing program (DE-FG02-06ER46290). The renewal proposal was submitted in November 2014, but because of confusion in the negotiations got issued as a new program. Subsequently, a correction was made where the new program (DE-SC0001450) was terminated, and a renewal to the existing program (DE-FG02-06ER46290) issued. About $8,000 was expended on the new program before the mistake was discovered, and actions begun to correct it. The Department of Materials Science and Engineering at Virginia Tech issued a 'Letter of Guarantee' to the University to continue work while the issues were sorted out.

The renewal proposal (DE-FG02-06ER46290) that was eventually funded was the same one as the new proposal (DE-SC0001450) that was initially funded. The $8,000 expended on the new proposal was subtracted from the eventual amount given in the renewal proposal.

Here, we submit the final report for this new program (DE-SC0001450) that was terminated. Since the Statement of Work was identical to the renewal proposal (DE-FG02-06ER46290), we submit to you as the final report for the new program (DE-SC0001450) the same information that we submitted as our annual report for DE-FG02-06ER46290 that was submitted to the program manager (Refik Kortan) in June 2016.

A. $BiFeO_3$ on Piezoelectric PMN-PT

One of the goals of this program is to induce the cycloidal to antiferromagnetic phase transition in $BiFeO_3$ (BFO) by epitaxial strain and external applied electric field (E). During this year, high-quality epitaxial BFO thin films were successfully deposited on $Pb(Mg_{1/3}Nb_{2/3})O_3$-30at%$PbTiO_3$

(PMN-30%PT) substrates by pulsed laser deposition (PLD). The effects of film thickness, laser energy density, and PMN-30PT substrate orientation on BFO epitaxial thin layers were systematically studied. In addition, structural studies under applied E have revealed induced strain transitions in BFO layers grown on (100) and (110) PMN-30PT.

Growth of $BiFeO_3$ on Piezoelectric PMN-PT: To optimize the deposition conditions, firstly BFO layers were deposited on $SrTiO_3$ (STO) and $LaAlO_3$ (LAO) substrates. Deposition conditions such as target-substrate distance, substrate temperature, oxygen partial pressure, pulse rate, annealing time, atmosphere, and etc., were studied by a series of experiments. Thin film x-ray diffraction (XRD), atomic force microscopy (AFM), and scanning electron microscopy (SEM) were employed to determine the crystal structure, surface morphology and film thickness, respectively. A $SrRuO_3$ (SRO) buffer layer was deposited between the BFO layer and the substrate, as an electrode by which to apply E onto the substrate. Even though SRO is not piezoelectric, this allowed us to optimize its deposition conditions.

Next, efforts were placed upon improving the techniques for obtaining smooth and polished PMN-PT substrates. A three-step polishing method was developed by which to obtain relatively smoother PMN-PT substrates with surface roughness less than 3nm (see Figs. 1A-C). To verify the substrates ferroelectric/piezoelectric transformation (or Curie) temperatures, temperature dependent dielectric constant measurements were performed, which was done before polishing so that the Au electrodes would be removed. This enabled us to know the substrate composition fairly accurately, as PMN-PT is a solid solution.

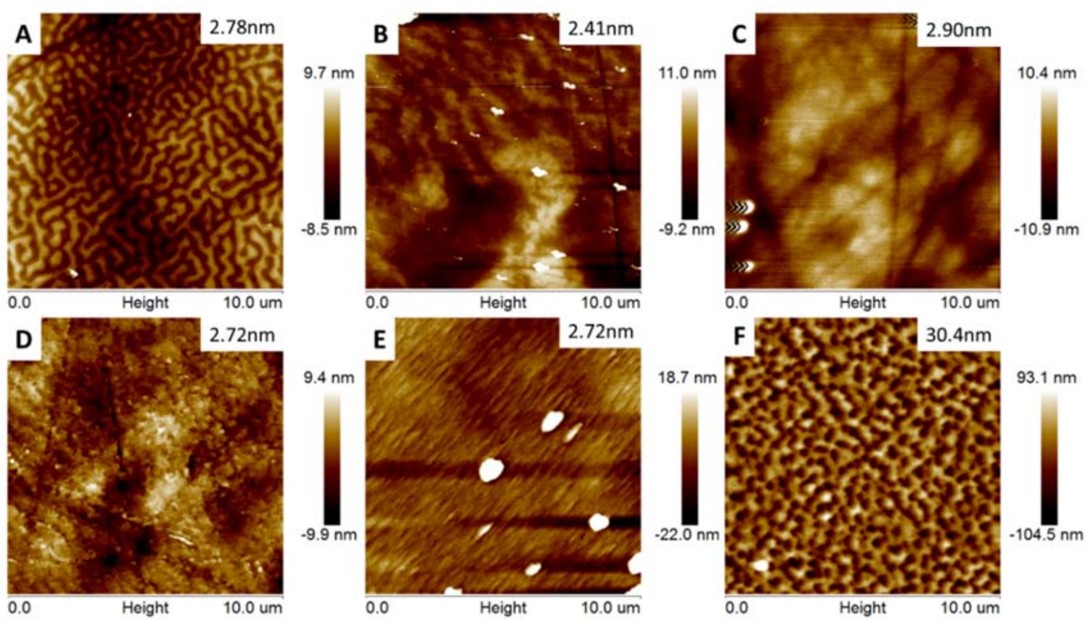

Figure 1. AFM images of (A)-(C) polished PMN30PT, and (D)-(F) BFO(50nm)/SRO(5nm)/ PMN30PT. The orientations of PMN-PT are (A)(D) (100), (B)(E) (110), and (C)(F) (111). The surface roughness is given in the inset.

After these prerequisite investigations, epitaxial BFO/SRO heterostructure layers were deposited on PMN-30PT. In order to tune the epitaxial strain of BFO, the effects of film thickness, laser energy density, and PMN-PT orientation were studied. Finally, an E-field was applied to the PMN-PT to change its lattice parameters via piezoelectricity, and the strain changes transferred to the BFO heterostructural layer were measured by XRD.

<u>Thickness and Laser Energy Density Effects on BFO:</u> Figures 2A and C show the effect of BFO and SRO layer thickness on the epitaxial strain of BFO. Although the laser energy densities are different (~3J/cm^2 in 2A and ~1J/cm^2 in 2C), the thickness effects exhibit the same trend. With increase of layer thickness for either the SRO (5nm to 20nm) or BFO (50nm to 100nm), the BFO peaks were shifted to lower 2θ values, indicating that the in-plane tensile strain of BFO decreases. The reason is that thicker SRO or BFO layers relax the strain of BFO.

Figure 2B shows the effect of laser energy density. As the energy density was reduced from 3J/cm^2 to 1.5J/cm^2, the strain of the BFO layer was fairly constant. However, on decreasing the energy density to below 1.15 J/cm^2, the tensile strain of the BFO layer was significantly increased to about 0.45%. Slower growth rates may allow for better epitaxy, and improve the quality of the BFO layer to some extent. According to Figs. 2A-C, BFO(50nm)/SRO(5nm) heterostructure layers deposited using a 1.00J/cm^2 laser energy density had the largest in-plane tensile strain.

Figure 2D shows the changes along the out-of-plane direction of the BFO(50nm)/SRO(5nm) heterostructure under application of E to (100) PMN-30PT. In order to calculate the in-plain strains, Gaussian fits were used to obtain the precise positions of the BFO peaks. Upon increasing the field from $0<E<9$kV/cm, the in-plane strain of BFO changed from 0.45% to 0.37%. Following the previously predicted epitaxial phase diagram of the spin states of BFO [1], this is close to the boundary between type-II cycloid and homogeneous antiferromagnetic states ($\varepsilon \approx 0.5\%$), as can be seen in Figure 3.

The E-induced changes to the in-plane strains of other heterostructure layers, such as BFO(70nm)/SRO(5nm) (Fig 2E) and BFO(50nm)/ SRO(10nm), were also measured (see Fig. 2F). The values of the BFO layer's in-plane strains were changed with increasing E up to 10kV/cm from 0.169% to 0.105%, and from tensile 0.076% to compressive -0.043%, respectively. Again, following the predicted epitaxial phase diagram of the spin states of BFO, the latter exactly changes across the boundary between type-I and type-II cycloid states (0%).

Accordingly, by tuning the thicknesses of the BFO and SRO layers, the in-plane strain of BFO was varied due to stress relaxation. By applying an out-of-plane E field modulation, the value of these in-plane strains were tuned across the predicted different magnetic phase boundaries. Hopefully, in the near future, we realize the E-induced cycloidal-antiferromagnetic phase transition of BFO, releasing the magnetoelectric interactions of BFO that are trapped within the spin cycloid.

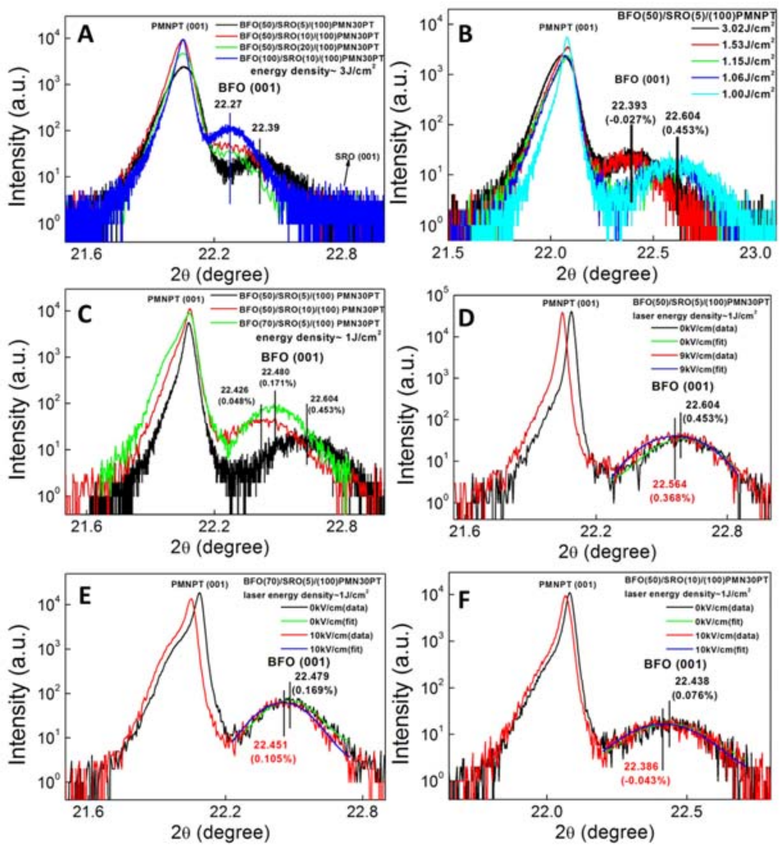

Figure 2. Thin film XRD patterns of BFO/SRO/(100)PMN30PT. (A),(C) thickness effects. (B) Laser energy density changed from 3.02 to 1.00J/cm2. (D)-(F) BFO samples with different thicknesses under E=0 and 10kV/cm, where the in-plane strains are given inside the brackets.

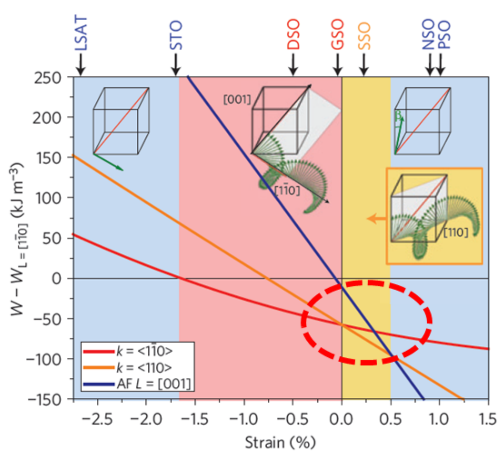

Figure 3. Magnetic phase diagram of strained BFO films. The stability of the different states are shown in colours (blue: homogeneous antiferromagnetic; red: type I cycloid; orange: type II cycloid). The different substrates used are located at the top of the diagram at their corresponding strain. [1] D. Sando, et al., Nature Materials 12, 641 DOI:10.1038/NMAT3629 (2013).

<u>*PMN-PT Orientation Effects on BFO :*</u> (110) and (111) PMN-30PT were then chosen as substrates upon which to deposit BFO(50nm)/SRO(5nm) heterostructure layers, with the goal of determining the orientation effects on BFO's strain. The layer deposition conditions were adjusted in a similar manner as for those grown on (100) PMN-PT, given above. The BFO layers on (110) PMN-30PT had similar surface roughness (see Fig. 1E) as that grown on (100) PMN-PT (see Fig. 1D). However, for BFO grown on (111) PMN-30PT, the surface roughness was notably larger, over 30nm (see Fig. 1F). This resulted in the quality of the films to be not as good for (111) BFO, as for the other two orientations, at least as characterized by XRD (see Fig. 3C).

Figures 4A and C show XRD patterns for BFO(50nm)/SRO(5nm) thin layers on (110) or (111) PMN-30PT, respectively, with E=0 and 10kV/cm applied to the PMN-PT substrates. Both (110) and (111) PMN-PT were found to have peak splittings, indicating phase coexistence of different ferroelectric phases near the morphotropic phase boundary. This resulted in the BFO layer on (110) PMN-PT having a doublet peak. By using Gaussian fits, the in-plane strains of the (110) BFO were found to change from 0.959% to 0.774% under 9.6kV/cm. These changes were larger than those for (100) BFO, both in magnitude and in variation.

Figures 4B and D show the lattice parameters of PMN-PT and in-plane strains of the BFO layer as a function of E for (110) and (100) BFO, respectively. The (110) BFO had relatively larger strains than the (100) one, but also had larger fluctuations under E due to peak splittings. However, the (100) BFO layer exhibited nice butterfly-shape curves with a coercive field near 2kV/cm, which is consistent with that of (100) PMN-30PT.

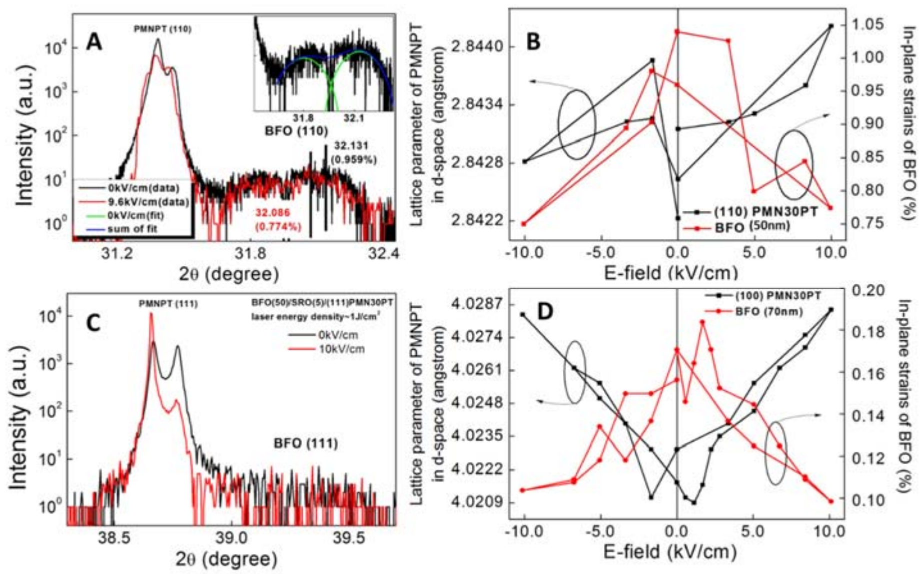

Figure 4. (A),(C) thin film XRD patterns of BFO(50nm)/SRO(5nm) on (A) (110) and (C) (111) PMN30PT with and without E-field. (B),(D) strains responses of BFO on (B) (110) and (D) (100) PMN30PT under various E-fields.

B. Self-biased magnetoelectric core-shell nanoparticles

Piezomagnetic and piezoelectric core-shell nanoparticles were synthesized by sol-gel and co-precipitation techniques. Piezoresponse force microscopy, magnetoelectric effect (ME) and magnetodielectric effect (MDE) measurements were conducted to evaluate the strength of magnetic-ferroelectric nanoscale interactions. Studies on magnetic field induced permittivity (ε′) and polarization (P) in core-shell nanoparticles showed an increase in ε′ and P due to tensile stress on the piezoelectric shell from a piezomagnetic core under magnetic field. The core-shell nanostructure demonstrated strong ferroelectric response with a saturation polarization, Ps, of 12 μC/cm^2, remnant polarization, Pr, of 8.7 μC/cm^2 and a coercive field Ec of 41 kV/cm. This resulted in strong magnetoelectric coupling coefficient of 242 mV/cm Oe at zero bias field and ac excitation filed of 1Oe. Magnetic and magnetodielectric behavior of core-shell nanocomposite are shown in Figure 1. Room temperature magnetization as a function of magnetic field H curves for NFO powder and NFO-PZT powder are 23 emu/g and 11.8 emu/g, respectively shown in Figure 5(a). The magnetization curves are not well saturated due to nanocrystalline behavior (~80nm). The possible reason for the decreased magnetic behavior in NFO sample compared to bulk samples (36 emu/g) is related to the large surface area by which the net magnetic moment is decreased due to weak dipole interaction. The magnetization value of 11.8 emu/g was obtained for core-shell nanoparticles which is estimated for ferrite weight fraction of 50% of 23 emu/g in NFO nanoparticles. The MDE measurements were conducted on a sintered sample with dimensions of 3x5 mm^2. Figures 5(b)-(c) shows the real part of the relative permittivity $\varepsilon_{r'}$ as a function of frequency from 1 kHz to 20MHz for zero and 3 kOe magnetic field. Both the curves show uniform increase of dielectric constant. We found a fractional increase in permittivity $\varepsilon_{r'}$ by 0.5 to 0.6% as a function of frequency at a magnetic field of 3kOe.

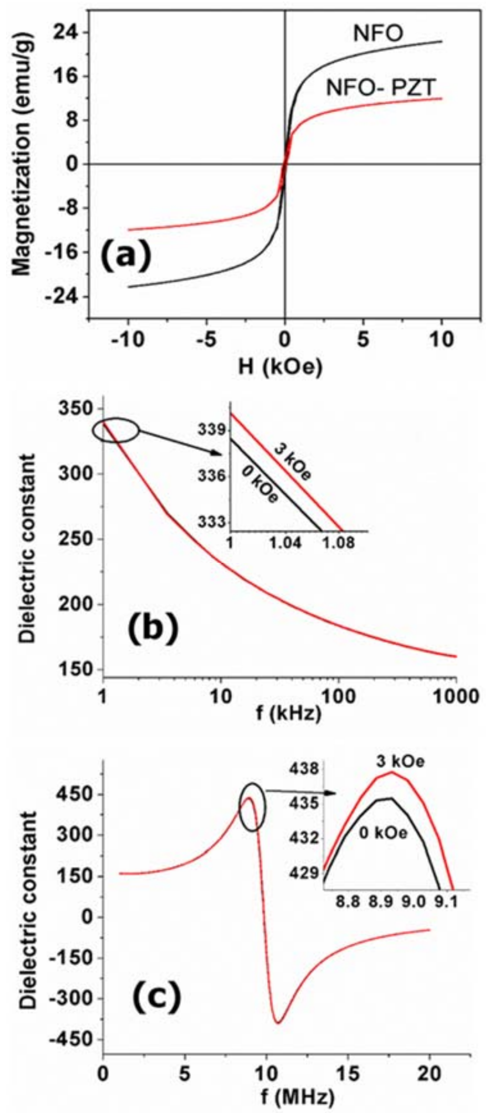

Figure 5. Magnetic and magnetodielectric behavior of core-shell nanostructures: (a) room temperature magnetization as a function of magnetic field H for NFO and NFO-PZT nanoparticles, and (b)-(c) real part of the relative permittivity εr' as a function of frequency for zero and 3 kOe magnetic field, both the curves shows uniform increase of dielectric constant, magnetodielectric behavior.

C. Tailoring the Magnetoelectric Properties of $Pb(Zr,Ti)O_3$ Film Deposited on Amorphous Metglas Foil by Laser Annealing

In this study we demonstrated the modulation of off-resonance ME response of the $Pb(Zr,Ti)O_3$ (PZT)/ Metglas (FeBSi) bilayered composite by laser annealing. A continuous-wave 532 nm Nd:YAG laser with varying fluences (210-390 J/mm^2) was utilized to anneal the 2 μm-thick PZT film deposited using granule spray in vacuum (GSV) technique on magnetostrictive amorphous Metglas foil. It was found that the dielectric and ferroelectric properties of the PZT film are strongly affected by the exposure to laser fluence. The ME voltage coefficient of PZT/Metglas increased with the fluence up to 345 J/mm^2, reaching a high value of 880 mV/cm·Oe. The electrical and ME properties were correlated with the changes observed in crystallinity and grain size of the PZT film as well as with the alterations in microstructure and magnetic behavior of Metglas. Our results demonstrate that enhanced ME coupling can be realized in PZT/Metglas film composites by controlling the laser fluence. Prior studies on some PZT-ferrite layered ME composites have demonstrated that interfacial chemical reactions between different phases during processing will reduce the ME coupling in the composite. In order to identify any atomic diffusion between PZT and Metglas due to laser irradiation, energy dispersive X-ray spectroscopy (EDS, equipped in TEM) analysis was conducted. Typical interface regions between PZT and Metglas layers, elemental distributions representing PZT and Metglas (contains Fe ~ 95 wt.%) phases, corresponding to the AD and 390 J/mm^2 LA conditions, are depicted in Figure 6. It can be seen from these images that the PZT film strongly adhered to Metglas and there was no obvious elemental diffusion across the PZT/Metglas interface before and after laser annealing. However, Metglas layer crystallized from laser irradiation of the composite at 390 J/mm^2. The findings of EDS analysis signify that the change in microstructure of Metglas alone could have caused the decrease in ME response of the composite annealed at 390 J/mm^2.

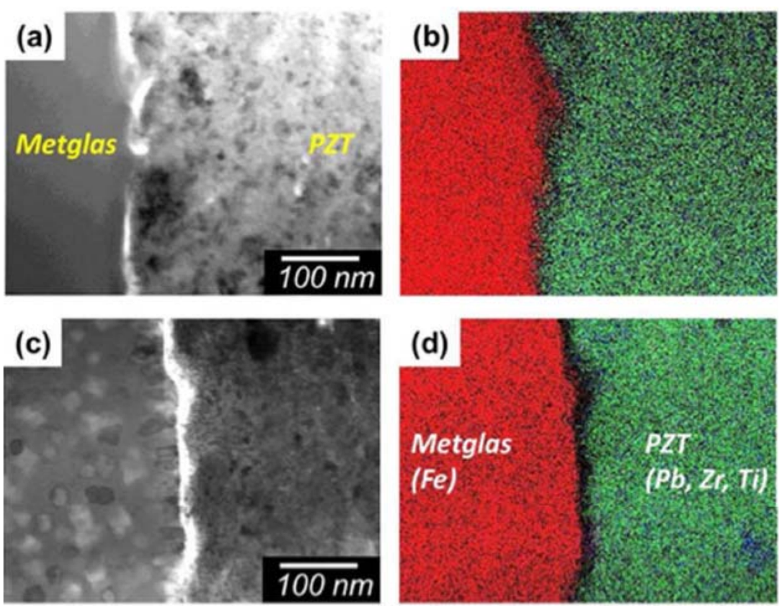

Figure 6: TEM cross-sectional images and corresponding summed up EDS elemental mappings of (a and b) as-deposited and (c and d) 390 J/mm^2 laser annealed PZT/Metglas composites. Here Fe, Pb, Zr, and Ti are shown in red, green, blue, and magenta colors, respectively.

Dielectric permittivity (ε) and dielectric loss factor (tan δ) measured as a function of frequency for the AD and LA PZT films on Metglas are presented in Figures 7(a) and (b), respectively. It can be seen that for all the samples, ε decreased gradually with increasing frequency while tan δ remained (below 10%) almost unchanged until exhibiting an increase in the high frequency range which is typical for ferroelectric materials including PZT. Higher values of ε and tan δ were obtained for the LA PZT films than the AD film. Despite the negligible changes observed for tan δ up to 100 kHz, there was a considerably large enhancement of ε (at f = 1 kHz) with increase in laser fluence. The polarization-electric field (P-E) hysteresis loops of the AD and LA PZT films are displayed in Fig. 7(c). The AD PZT film exhibited a much slim and unsaturated hysteresis loop with incipient polarization switching, similar to a paraelectric material. In case of LA PZT films, the remnant (P_r) and saturated (P_s) polarization values and the hysteretic nature of the P-E loop was improved as the laser fluence increased. The results of dielectric and ferroelectric characterization of the AD and LA PZT films on Metglas obtained herein are consistent with those reported for furnace annealed and laser irradiated polycrystalline $Pb(Zr_{0.52}Ti_{0.48})O_3$ thick films. The above results can be explained on the basis of microstructural changes caused by laser irradiation of PZT. The frozen dipolar regions in amorphous PZT formed by distortion of Zr/Ti-O_6 octahedra, become active upon crystallization. The low values of permittivity and polarization of AD PZT film may be attributed to the larger content of non-polar amorphous phase present in the volume. The enhancements in these values for LA PZT films indicate the increase in fraction of the ferroelectric PZT phase due to the crystallinity improvement and grain growth with increase in laser fluence. The increased crystallinity reduces the short-range repulsion forces and stabilizes the ferroelectric phase while grain growth promotes the domain wall motion and switching both of which contribute to the enhancement of the dielectric and ferroelectric properties. The microstructural changes induced by laser irradiation of PZT/Metglas was further investigated by TEM analysis. The ME coupling recorded from PZT/Metglas composite annealed using different laser fluences are displayed in Figure 7(d). All the samples showed the typical α_{ME} vs. H_{dc} characteristic and exhibited maximum α_{ME} values below a H_{dc} of 50 Oe in off-resonance mode (H_{ac} = 1 Oe and f = 1 kHz). The ME coefficient increased with increase in laser fluence up to 345 J/mm^2 and decreased thereafter, contrary to the changes in dielectric and ferroelectric properties with laser fluence. Moreover, processing under higher laser fluence (345 and 390 J/mm^2) resulted in changes in ME behavior and position of maximum α_{ME} possibly due to the alteration in magnetic properties of Metglas. The improvement in α_{ME} until a laser fluence of 345 J/mm^2 is solely due to the corresponding increase in piezoelectric performance of the PZT film while the decrement in α_{ME} at 390 J/mm^2 may be ascribed to the changes in Metglas substrate. The maximum α_{ME} of 880 mV/cm·Oe at a bias field of 25 Oe was obtained for the sample annealed with 345 J/mm^2.

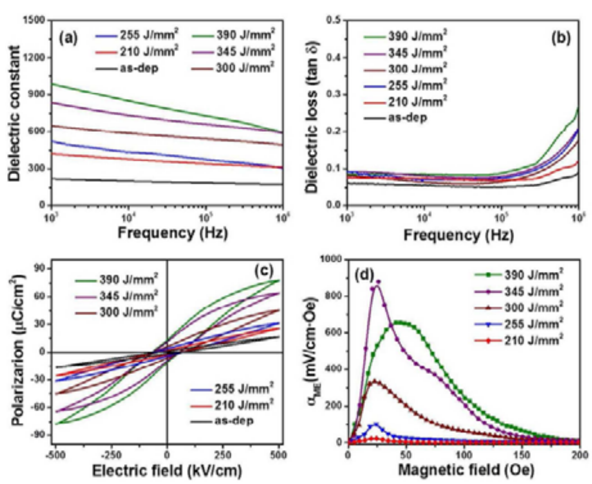

Figure 7. (a) and (b) Dielectric constant and loss tanδ, (c) Polarization-electric field (P-E) curves of as-deposited and laser annealed PZT/Metglas, and (d) ME voltage coefficient (αME)dependence of applied magnetic field (*Hdc*) under a constant AC magnetic field condition of 1Oe at *f*=1 kHz for laser annealed PZT/Metglas.

5. A list of papers (already published, in press) in which DOE support is acknowledged.

1) Haribabu Palneedi, Insung Choi, Gi-Yeop Kim, Venkateswarlu Annapureddy, Deepam Maurya, Shashank Priya, Jong-Woo Kim, Keon Jae Lee, Si-Young Choi, Sung-Yoon Chung, Suk-Joong L. Kang and Jungho Ryu, "Tailoring the Magnetoelectric Properties of $Pb(Zr,Ti)O_3$ Film Deposited on Amorphous Metglas Foil by Laser Annealing", J. Amer. Ceram. Soc., DOI: 10.1111/jace.14270 (2016).
2) Haribabu Palneedi, Venkateswarlu Annapureddy, Shashank Priya and Jungho Ryu, "Status and Perspectives of Multiferroic Magnetoelectric Composite Materials and Applications", *Actuators* **2016**, *5*(1), 9; doi:10.3390/act5010009
3) G. Sreenivasulu, Y. Yan, D. Maurya, M. Sanghadasa and S. Priya, "Self-bias magnetoelectric core-shell nanoparticles", Nanotechnology (2016), to be submitted.
4) Min Gyu Kang, Seul-Yi Lee, Deepam Maurya, Christopher Winkler, Hyun-Cheol Song, Robert B. Moore, Mohan Sanghadasa and Shashank Priya, "Large area close-packed single crystalline ferroelectric nanorod arrays on silicon", Nature Comm. (2016), under review.

6. A list of people working on the project -graduate students, postdocs, visitors, technicians, etc. Indicate for each whether receiving full or partial support. In case of partial support indicate percentage of support.

Sreenivasulu Gollapudi (postdoc)
Han-Byul Kang (Ph.D. student)
Min Gao, Graduate Student

7. Planned activities for next year, which could be a short paragraph.

We plan to study the magnetic properties of BFO under different applied electric fields. We will use a vibrating sample magnetometer (VSM), superconducting quantum interference device (SQUID), and/or neutron diffraction to study the strain-mediated E-induced magnetic phase transitions of BFO.

Currently, we are also developing the experimental plan to utilize core-shell nanoparticles for synthesis of the ME films on the Metglas foil. Thermal models including the band structure of NFO, PZT and Metglas are being developed to identify the dimensions and dopants that will facilitate coupling between the magnetic and ferroelectric domains. Based upon the guidance provided by the model, we will initiate GSV deposition and laser annealing experiments.

8. **Expenditure plan:**

There will be more than 10% funds will remaining at the end of the annual funding period, but less than 25%. The reason for the funds not being obligated is do to the confusion regarding contract negotiations, resulting in a delay of 7-8 months. Work was continued for that time period only because of a Letter of Guarantee issued by the Department. Accordingly, we are running behind in our investigations and expenditures.

9. An update list of other support (current and pending, federal and non-federal.) For each, indicate the overlap, if any, and/or distinctiveness with the DOE-supported project. This could be brief - one or two sentences.

Dwight Viehland

Support: ☒ Current ☒ Pending ☐ Submission Planned in Future ☐ *Transfer of Support

Project/Proposal Title: ORNL GO! Networking Workshop (40000135182)
Source of Support: ORNL
Total Award Amount: $60262 Total Award Period Covered: 10/1/14-7/1/2016
Location of Project:
Person-Months Per Year Committed to Project. Cal: Acad: 0 Sumr: 0

Support: ☒ Current ☒ Pending ☐ Submission Planned in Near Future ☐ *Transfer of Support

Project/Proposal Title: Mesoscale interfacial dynamics in magnetoelectric nanocomposites (*LOG-LOG-DE-FG02-06ER46290*)
Source of Support: Department of Energy
Total Award Amount: $1,238,882 Total Award Period Covered: 8/2006-7/2018
Location of Project: Virginia Tech
Person-Months Per Year Committed to the Project. Cal: Acad: Sumr:

Support: ☒ Current ☐ Pending ☐ Submission Planned in Near Future ☐ *Transfer of Support

Project/Proposal Title: A MATRIX Solution to Solid State Devices for Scalable, Integratable, and Efficient Signal and Power Processing (W911NF-15-1-0616)
Source of Support: Office of Naval Research
Total Award Amount: $1,500,000 Total Award Period Covered: 10/1/2015-9/30/2016
Location of Project: Virginia Tech
Person-Months Per Year Committed to the Project. Cal: Acad: Sumr:

Support: ☒ Current ☐ Pending ☐ Submission Planned in Near Future ☐ *Transfer of Support

Project/Proposal Title: Reconfigurable electronics based on multi-ferroics and nano-magnetism Electronics (FA9550-16-1-0001)
Source of Support: Department of Defense
Total Award Amount: $812,298.00 Total Award Period Covered: 4/1/2015-3/30/2020
Location of Project: Virginia Tech
Person-Months Per Year Committed to the Project Cal: Acad: 0 Sumr:

Support: ☒ Current ☐ Pending ☐ Submission Planned in Near Future ☐ *Transfer of Support

Project/Proposal Title: Rare Earth Free Magnetostrictive (N00014-13-1-0049)
Source of Support: Office of Naval Research
Total Award Amount: $360,000 Total Award Period Covered: 12/2012-11/2016
Location of Project: Virginia Tech
Person-Months Per Year Committed to the Project. Cal: Acad: Sumr:

Support: ☒ Current ☐ Pending ☐ Submission Planned in Near Future ☐ *Transfer of Support

Project/Proposal Title: Magnetic Sensors for Detection (N00014-15-1-2457)
Source of Support: Office of Naval Research
Total Award Amount: $300,000 Total Award Period Covered: 7/2015-6/2018
Location of Project: Virginia Tech
Person-Months Per Year Committed to the Project. Cal: Acad: Sumr:

Support: ☐ Current ☐ Pending ☒ Submission Planned in Future ☐ *Transfer of Support

Project/Proposal Title: Adaptive Design and Discovery of Materials: Controlling Functionality at the Mesoscale
Source of Support: LANL
Total Award Amount: Total Award Period Covered:
Location of Project:
Person-Months Per Year Committed to Project. Cal: 0.3 Acad: 0 Sumr: 0

Shashank Priya

Current and Pending Support

(See GPG Section II.C.2.h for guidance on information to include on this form.)

The following information should be provided for each investigator and other senior personnel. Failure to provide this information may delay consideration of this proposal.

Investigator: Shashank Priya

Other agencies (including NSF) to which this proposal has been/will be submitted.

Support: ☒ Current ☐ Pending ☐ Submission Planned in Near Future ☐ *Transfer of Support
Project/Proposal Title: Nano Engineered Thermoelectric Systems (NETS) for Lightweight Portable Primary/Secondary Power Sources

Source of Support: DARPA
Total Award Amount: $ 4,345,935 Total Award Period Covered: 09/01/15 - 08/31/18
Location of Project: Virginia Tech
Person-Months Per Year Committed to the Project. Cal:0.00 Acad: 0.45 Sumr: 1.00

Support: ☐ Current ☒ Pending ☐ Submission Planned in Near Future ☐ *Transfer of Support
Project/Proposal Title: DURIP: 2D scanning laser vibrometer for research on high efficiency dual-phase energy harvesters and CNT acoustic transducers

Source of Support: ONR
Total Award Amount: $ 311,095 Total Award Period Covered: 07/01/16 - 06/30/17
Location of Project: Virginia Tech
Person-Months Per Year Committed to the Project. Cal:0.00 Acad: 0.00 Sumr: 0.00

Support: ☒ Current ☐ Pending ☐ Submission Planned in Near Future ☐ *Transfer of Support
Project/Proposal Title: Tunable Energy Efficient Electronics (TE3)

Source of Support: DARPA
Total Award Amount: $ 3,998,874 Total Award Period Covered: 09/01/15 - 08/31/18
Location of Project: Virginia Tech
Person-Months Per Year Committed to the Project. Cal:0.00 Acad: 0.45 Sumr: 0.90

Support: ☐ Current ☒ Pending ☐ Submission Planned in Near Future ☐ *Transfer of Support
Project/Proposal Title: CREST - Center for Renewable Energy and Advanced Materials (CREAM)

Source of Support: Norfolk State University / NSF
Total Award Amount: $ 150,000 Total Award Period Covered: 07/01/15 - 06/30/18
Location of Project: Virginia Tech
Person-Months Per Year Committed to the Project. Cal:0.00 Acad: 0.00 Sumr: 0.50

Support: ☐ Current ☒ Pending ☐ Submission Planned in Near Future ☐ *Transfer of Support
Project/Proposal Title: PICO: Bubble Chambers for Dark Matter Dectection

Source of Support: University of Chicago / NSF
Total Award Amount: $ 398,690 Total Award Period Covered: 08/01/16 - 07/31/17
Location of Project: Virginia Tech
Person-Months Per Year Committed to the Project. Cal:0.36 Acad: 0.00 Summ: 0.00

*If this project has previously been funded by another agency, please list and furnish information for immediately preceding funding period.

Page G-1 USE ADDITIONAL SHEETS AS NECESSARY

Current and Pending Support

(See GPG Section II.C.2.h for guidance on information to include on this form.)

The following information should be provided for each investigator and other senior personnel. Failure to provide this information may delay consideration of this proposal.

Investigator: Shashank Priya

Other agencies (including NSF) to which this proposal has been/will be submitted.

Support: ☒ Current ☐ Pending ☐ Submission Planned in Near Future ☐ *Transfer of Support
Project/Proposal Title: Mesoscale Design of Magnetoelectric Heterostructures and Nanocomposites

Source of Support: DOE
Total Award Amount: $ 563,736 Total Award Period Covered: 08/01/15 - 07/31/18
Location of Project: Virginia Tech
Person-Months Per Year Committed to the Project. Cal:0.00 Acad: 0.18 Sumr: 0.15

Support: ☒ Current ☐ Pending ☐ Submission Planned in Near Future ☐ *Transfer of Support
Project/Proposal Title: NonLinear and Terahertz Studies of Electro-Optic and Magnetoelectric Materials

Source of Support: AFOSR
Total Award Amount: $ 1,199,998 Total Award Period Covered: 09/30/14 - 09/29/17
Location of Project: Virginia Tech
Person-Months Per Year Committed to the Project. Cal:0.15 Acad: 0.00 Sumr: 0.00

Support: ☒ Current ☐ Pending ☐ Submission Planned in Near Future ☐ *Transfer of Support
Project/Proposal Title: Textured Ceramic Samples for Testing

Source of Support: ONR NUWC Newport
Total Award Amount: $ 10,007 Total Award Period Covered: 01/01/16 - 09/30/16
Location of Project: Virginia Tech
Person-Months Per Year Committed to the Project. Cal:0.12 Acad: 0.00 Sumr: 0.00

Support: ☐ Current ☒ Pending ☐ Submission Planned in Near Future ☐ *Transfer of Support
Project/Proposal Title: Self-biased dual stimulation (vibration+magnetic field) energy harvester for wireless structural health monitoring sensor nodes

Source of Support: ONR
Total Award Amount: $ 240,000 Total Award Period Covered: 05/01/16 - 04/30/19
Location of Project: Virgina Tech
Person-Months Per Year Committed to the Project. Cal:0.48 Acad: 0.00 Sumr: 0.00

Support: ☐ Current ☒ Pending ☐ Submission Planned in Near Future ☐ *Transfer of Support
Project/Proposal Title: Smart Robotics and Automation for Anterior Cruciate Ligament Reconstruction

Source of Support: NIH
Total Award Amount: $ 437,212 Total Award Period Covered: 07/01/16 - 06/30/18
Location of Project: VirginiaTech
Person-Months Per Year Committed to the Project. Cal:0.76 Acad: 0.00 Summ: 0.00

*If this project has previously been funded by another agency, please list and furnish information for immediately preceding funding period.

Current and Pending Support

(See GPG Section II.C.2.h for guidance on information to include on this form.)

The following information should be provided for each investigator and other senior personnel. Failure to provide this information may delay consideration of this proposal.

Investigator: Shashank Priya

Other agencies (including NSF) to which this proposal has been/will be submitted.

Support: ☐ Current ☒ Pending ☐ Submission Planned in Near Future ☐ *Transfer of Support
Project/Proposal Title: Development of Composite Multifunctional Piezoelectric Paving Materials for Energy

Source of Support: Univ of Science & Technology Beijing China
Total Award Amount: $ 76,969 Total Award Period Covered: 06/01/16 - 12/31/21
Location of Project: Virginia Tech
Person-Months Per Year Committed to the Project. Cal:0.00 Acad: 0.00 Sumr: 0.00

Support: ☐ Current ☒ Pending ☐ Submission Planned in Near Future ☐ *Transfer of Support
Project/Proposal Title: Understanding Thermamagnetic Instabilities in the Context of Energy Harvesting

Source of Support: UCLA - US DOE Office of Science
Total Award Amount: $ 300,000 Total Award Period Covered: 10/01/16 - 09/30/19
Location of Project: Virginia Tech
Person-Months Per Year Committed to the Project. Cal:0.40 Acad: 0.00 Sumr: 0.00

Support: ☐ Current ☒ Pending ☐ Submission Planned in Near Future ☐ *Transfer of Support
Project/Proposal Title: CPS: Synergy: Collaborative Research: Closed Loop Sustainable Precision Animal Agriculture

Source of Support: NSF
Total Award Amount: $ 687,673 Total Award Period Covered: 01/09/17 - 01/08/20
Location of Project: Virginia Tech
Person-Months Per Year Committed to the Project. Cal:0.60 Acad: 0.00 Sumr: 0.00

Support: ☐ Current ☒ Pending ☐ Submission Planned in Near Future ☐ *Transfer of Support
Project/Proposal Title: STTR: Phase II: High Temperature Piezoelectric Materials for Co-Fired Multilayer Devices

Source of Support: Prime Photonics
Total Award Amount: $ 250,000 Total Award Period Covered: 11/01/16 - 10/31/18
Location of Project: Virginia Tech
Person-Months Per Year Committed to the Project. Cal:0.30 Acad: 0.00 Sumr: 0.00

Support: ☐ Current ☒ Pending ☐ Submission Planned in Near Future ☐ *Transfer of Support
Project/Proposal Title: STTR Phase I:Development of Power Autonomous AMBS (Activity Monitor and Blood Sampler)

Source of Support: OptiXtal
Total Award Amount: $ 93,874 Total Award Period Covered: 01/01/17 - 12/31/17
Location of Project: Virginia Tech
Person-Months Per Year Committed to the Project. Cal:0.60 Acad: 0.00 Summ: 0.00

*If this project has previously been funded by another agency, please list and furnish information for immediately preceding funding period.